

Where heat adaptation is needed most - an open-source approach to developing a transferable heat risk index for urban planning

Saskia Rupp, Tobias Leichtle, Christoph Beck, Michael Hiete

Angaben zur Veröffentlichung / Publication details:

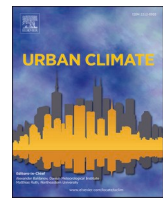
Rupp, Saskia, Tobias Leichtle, Christoph Beck, and Michael Hiete. 2026. "Where heat adaptation is needed most - an open-source approach to developing a transferable heat risk index for urban planning." *Urban Climate* 65: 102769.

<https://doi.org/10.1016/j.ulclim.2025.102769>.

Nutzungsbedingungen / Terms of use:

CC BY 4.0





Where heat adaptation is needed most - An open-source approach to developing a transferable heat risk index for urban planning



Saskia Rupp ^{a,b,*}, Tobias Leichtle ^c, Christoph Beck ^b, Michael Hiete ^a

^a Ulm University, Institute of Theoretical Chemistry, Helmholtzstraße 18, 89081 Ulm, Germany

^b Augsburg University, Institute of Geography, Alter Postweg 118, 86159 Augsburg, Germany

^c German Aerospace Centre (DLR), German Remote Sensing Data Centre (DFD), Münchner Straße 20, 82234 Weßling, Germany

ARTICLE INFO

Keywords:

Heat risk index
Urban heat stress
Latent class analysis
Heat risk management
Urban health
Heat risk patterns

ABSTRACT

With rising temperatures and ongoing demographic shifts, heat-related health risks are expected to intensify in the coming decades, highlighting the need for tailored adaptation and mitigation strategies – especially in densely populated urban areas. This study presents a transferable approach for constructing a Heat Risk Index (HRI) using open-source data and tools to support urban stakeholders in identifying and addressing heat vulnerability. The HRI integrates climatological data (hazard), population distribution (exposure), and socio-demographic factors (sensitivity) to assess spatial heat risk patterns across urban areas. Within three model cities, population groups were identified by conducting a Latent Class Analysis (LCA) based on social vulnerability data. Three latent classes (LCs) were consistently found across cities: "Young & Diverse", "Adults & Citizens" and "Elderly & Single-Household". Heat risk was distributed unevenly among these groups and spatially within each city. By mapping both heat exposure and social vulnerability, the study offers a practical tool for risk mitigation in urban planning. While this approach enhances understanding heat-related vulnerability, it faces limitations related to data resolution, model assumptions, and static representations of risk. Further research should explore whether similar risk groups can be identified across multiple cities, or whether variations in urban structure – such as infrastructural and social – lead to different patterns of heat risk within cities. Additionally, adapting the HRI to different seasons or daytimes or developing personas for each population group to establish a more advanced planning tool for local stakeholders in heat risk management could be a different future research approach.

1. Introduction

As a consequence of climate change, extreme heat events are expected to increase in intensity, frequency and duration while simultaneously affecting a greater geographical expanse in the near future (e.g., [Jay et al., 2021](#); [Paterson and Godsmark, 2020](#)). Thus, the risk of suffering from a variety of heat-related physical and mental health issues such as fatigue, heat stroke or even death (e.g., [Ebi et al., 2021](#)) will increase for a significant proportion of the world's population ([IPCC, 2023](#)). For example, between 2014 and 2023 approximately 48,000 deaths were related to heat ([W et al., 2024](#)). Due to changes in demography ([Ebi et al., 2021](#)) as well as increasing air temperature ([Jay et al., 2021](#)), heat-related deaths will most likely increase within Germany in the future ([W et al., 2024](#)).

* Corresponding author at: Ulm University, Institute of Theoretical Chemistry, Helmholtzstraße 18, 89081 Ulm, Germany.

Besides the climatological factors such as air temperature, air humidity or air flow social factors also influence heat-related health risk (e.g., European Environment Agency, 2022). For instance, a person's sensitivity towards heat is influenced by age (e.g., Cheng et al., 2018), chronic or acute illnesses such as diabetes or cardiovascular diseases (e.g., Kenny et al., 2010; Saucy et al., 2021), lifestyle such as being an outdoor worker (e.g., Herrmann and Sauerborn, 2018; Seebaß, 2017), level of autonomy (e.g., Hass and Ellis, 2019; Herrmann and Sauerborn, 2018) and an individuals' financial (e.g., Jay et al., 2021) or social capital (Hass and Ellis, 2019) – meaning the individuals' social support an individual perceives from their social surrounding (Wolf et al., 2010). Heat adaptation measures can reduce heat-related mortality and morbidity (Ebi et al., 2021). For instance, institutional changes such as improving or reorganizing medical care options and reachability as well as awareness might reduce heat-related health risk (e.g., Bernhard et al., 2015; Frasch et al., 2025; Masselot et al., 2025). Besides individual adaptation measures such as an increase in water intake, limiting physical activity or adapting one's time schedule (e.g., Ebi et al., 2021), urban planning can also reduce individual heat risk. For instance, redesigning or planting of green infrastructure as well as implementing or extending blue infrastructure, modern building concepts or the installation of shading objects and drinking fountains (e.g., Jay et al., 2021) can enhance individual adaptation behaviour.

Heat Risk Indexes (HRIs) visualized in form of heat risk maps can support various stakeholders involved in urban planning processes to implement suitable heat risk adaptation and mitigation measures in order to reduce inhabitants' thermal stress (Jay et al., 2021). The development of HRIs that consider individual factors to measure and identify heat risk has increasingly become a subject of scientific literature (e.g., Boumans et al., 2014; Depietri et al., 2013), on a regional (e.g., Abrar et al., 2022; Alonso and Renard, 2020) or nation-wide (e.g., Georgy et al., 2019; Huang et al., 2020) scale. Many studies on HRIs struggle with representing social factors influencing individual heat risk for instance due to data availability and accuracy as well as high monetary and time expenses (e.g., Klopfer and Pfeiffer, 2023; Pappalardo et al., 2023; Sun et al., 2022).

To detect homogenous subgroups within a dataset, Latent Class Analysis (LCA) has been used in multiple contexts as for instance examining individual's perceptions (e.g., Barnes et al., 2013), attitudes towards technologies (e.g., Ferguson et al., 2018) or climate change beliefs (e.g., Kácha et al., 2022; Korkala et al., 2014) as well as health-related topics such as tobacco use (e.g., Nguyen et al., 2024) or asthma characteristics (e.g., Keller et al., 2024). In some studies, LCA supported the local disaster risk management. For instance, Bodoque et al. (2016) assessed locals' awareness of civil protection and emergency management in regard of flash floods and combined this information with hydrological and hydraulic models in order to establish different types of flash flood risk preparedness. Pinchoff et al. (2024) classified climate vulnerability and inequalities in three different countries with the help of LCA.

A municipality's heat adaptation and mitigation strategies may succeed or fail depending on the population structure. While implementing sociodemographic information into HRI construction has been explored in the past (e.g., Boumans et al., 2014; Depietri et al., 2013), this study aims to support urban heat risk management by proposing a transferable methodological approach to visualize heat risk and its interrelationship with social vulnerability. Different sociodemographic characteristics influence the extent to which individuals benefit from specific heat risk mitigation and adaptation strategies. For example, some population groups might benefit highly from redesigning green spaces, whereas others' health might be more strongly supported by implementing and promoting social control mechanisms during heat events. Therefore, tailored solutions in urban planning are essential for achieving the most effective cost-benefit outcomes in local planning contexts. This study's key contribution lies in creating sociodemographically homogenous groups through LCA and combining them with heat risk index (HRI) construction, thereby enabling the design and implementation of tailored mitigation and adaptation measures while supporting local decision-makers. The high spatial resolution of 100 m × 100 m provides detailed insights into local heat patterns, thereby facilitating the precise identification of urban heat hotspots and the implementation of targeted mitigation and adaptation measures at the neighbourhood scale. Another strength of this study is that, by relying on open-source datasets and software, the proposed method is both reproducible and accessible for local stakeholders.

In order to address these considerations two research goals (RGs) have been established:

RG1. *Identifying spatial patterns of heat risk across the three model cities.*

RG2. *Identifying population groups with varying heat sensitivity to support targeted adaptation and mitigation measures.*

Two specific research questions (RQs) were derived from the previously set RGs:

RQ1. *How does heat stress affect different population groups in the urban areas of each model city?*

RQ2. *What spatial patterns can be observed for high-risk population groups within and across the three model cities?*

To answer these research questions, this study combines sociodemographically homogenous subgroups with a heat risk index (HRI) to assess both population-specific and spatial patterns of heat vulnerability and to support targeted adaptation strategies. These subgroups were identified through latent class analysis (LCA) using open-source census data at 100 m × 100 m resolution. Each census data area was assigned to a latent class (LC), allowing for a nuanced representation of population groups with differing heat sensitivities. LCA was chosen as it results in a proportional classification rather than providing disjoint classes such as most clustering methods (e.g., k-means). And, due to the probabilistic model-based approach, goodness of fit can be evaluated among different models with different numbers of latent classes (Sinha et al., 2021), giving stakeholders insight into the certainty of class assignments. Additionally, LCA accommodates mixed data types, enabling integration of multiple indicators that capture diverse aspects of heat sensitivity (Sinha et al., 2021). Combining these sociodemographic data with an HRI allows municipal and planning stakeholders to incorporate social vulnerability into urban heat risk management and thus, to implement targeted, context-specific adaptation strategies at the local scale.

2. Methodological approach

An LCA was conducted to identify subsets of homogenous groups within the model cities' populations. Subsequently, an HRI was developed including climatological variables (hazard index), in situ population (exposure index) and social factors leading to heat risk (sensitivity index). Finally, interrelationships between HRI index values and latent classes were evaluated. In the following the multimethod-approach used for this study is displayed in more detail.

2.1. Study area

Study sites were chosen due to stakeholder contacts and cooperation in the context of the HEATS-project (Heat Risk Management in the City). [Table 1](#) shows the characteristic of all three study sites.

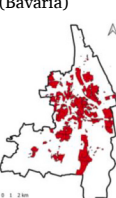
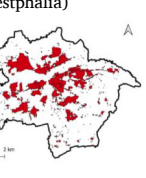
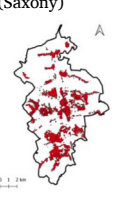
2.2. LCA

LCA can be used to detect homogenous subgroups within a dataset that exhibits no obvious natural clustering ([Sinha et al., 2021](#)). It identifies underlying homogeneous subgroups within a larger heterogeneous group with a probabilistic model and generates an affiliation probability towards a latent class for each data point within the original dataset. During the last years, LCA has been applied in various research fields (e.g., psychology ([Coid et al., 2021](#)) or behavioural science ([Nguyen et al., 2024](#))) but was rarely used in risk management. For instance, [Bodoque et al. \(2016\)](#) employed an LCA in the context of flash-flood risk management by assessing individuals' perceptions as well as their awareness of flooding events and protection and emergency management measures. This information was combined with more classical methods of flood risk modelling (in this case: establishing hydrological and hydraulic models). As shown by [Bodoque et al. \(2016\)](#) combining LCAs with established approaches of risk management research might enhance the understanding of spatial risk patterns within a city or municipality by providing new perspectives on and allowing the introduction of different types of data to risk management.

In this study, different types of households, each distinctly characterized by various heat risk factors were identified using LCA. The data foundation were the latest national census data for 2022 from Germany provided with open access by the [German Federal Statistics Office \(2024a\)](#). In this context data on age (> 65 years and < 10 years) ([Cheng et al., 2018; Ebi et al., 2021; Seebaß, 2017](#)), household size ([Hass and Ellis, 2019](#)), net rent ([Kenny et al., 2010](#)) and share of foreign population (here: birthplace ≠ Germany) ([Ebi et al., 2021](#)) were used in the LCA. While the indicator age is typically linked to an inherent physiological vulnerability, household size, net rent and share of foreign population are taken as proxies for adaptive capacity. For instance, individuals in multi-person

Table 1

Description of Study Sites. Source: [German Federal Statistics Office \(2024b\)](#): inhabitants, city area, population density, average cost for rent, average inhabitant age, higher education diploma, unemployment rate. [DWD \(2025\)](#): annual mean temperature, average summer days, average hot days, annual precipitation. Mean data refers to the period: 01.01.1981–31.12.2010. DWD stations: Augsburg “Augsburg”; Hamm “Station Bad Lippspringe”, Zwickau “Leipzig Flughafen”.

	Augsburg	Hamm	Zwickau
Location	Southern Germany (Bavaria)	Western Germany (North Rhine Westphalia)	Eastern Germany (Saxony)
			
Population	294,647 inhab.	179,070 inhab.	87,020 inhab.
City area	146.85 km ²	226.42 km ²	102.58 km ²
Population density	2006 inhab. /km ²	791 inhab. /km ²	848 inhab. /km ²
Annual mean temperature	10.6 °C (2024)	11.4 °C (2024)	11.7 °C (2024)
Average summer days (Tmax ≥ 25 °C)	39.3	30.5	42
Average hot days (Tmax ≥ 30 °C)	6	5.8	8.5
Annual precipitation	767.1 mm	951 mm	534.3 mm
Average cost of rent (2024)	8.48 €/m ²	5.75 €/m ²	5.20 €/m ²
Higher education diploma (share of individuals with)	24.5 %	12.8 %	16.1 %
Unemployment rate	4.6 %	4.2 %	2.9 %

households are likely to perceive higher social control than individuals living in single-households. Individuals born within Germany might face less barriers regarding cultural or language barriers (e.g., access to information, comprehension of heat warnings, social networks, etc.) while high net rents might indicate higher financial resources which facilitates an individual's adaptive capacity by providing access to air conditioning or paying for entry fees to cool places (e.g., public swimming pool, cafés, etc.). Further information on input data and sources is depicted in Table A1 in the appendix. The decision on which data to include as indicators in the LCA was based on data availability and information retrieved from current scientific literature. Following the recommendation by [SINHA ET AL. \(2021\)](#) continuous variables were categorized according to the same pattern, resulting in a three-category representation (below average, average, above average). These categories were chosen in order to provide clearly defined categories for subsequent interpretation. Also, these categories allow a stringent presentation of the results for all three model cities. However, while the categories were identical, the exact cut off values were adapted for each model city. Standardized categories for all three model cities were not practicable due to different lifestyle levels (e.g., rent levels, demographic structures, immigration and emigration levels in Southern Germany vary greatly from rent levels in Eastern Germany) between the cities and the goal of the study to provide information on heat risk in context of one municipality rather than on a national scale. To ensure usability for local planning stakeholders and support a customized city planning on neighbourhood level, the highest available spatial resolution (100 m × 100 m) provided by the [German Federal Statistics Office \(2024a\)](#) was chosen. Geolocation was used as an identification key. In the case of one missing information, the datapoint was removed, which was necessary in order to conduct the LCA and ensure a more realistic result.

LCA allows researchers to detect homogenous subgroups within an existing population through a probabilistic model ([Sinha et al., 2021](#)). The LCA in this study was realised with the poLCA package in R using the default function ([Linzer and Lewis, 2011](#); [Linzer and Lewis, 2013](#)). Several variants of LCA have been performed. Based on Bayesian Information Criterion (BIC), Akaike Information Criterion (AIC), entropy, class size, precision of class affiliation (share of posterior probabilities with a precision $\geq 90\%$) and logical fit the best fitting latent class model was chosen and the risk of false model choice was minimized. As this study has the aim to produce results which can be used in practice by the model municipality administration, we also considered class size (due to practicability in implementing heat-risk-management measures) when choosing the best fitting LC model for each study case. Model fit was given by the following fit indices, elaborated in more detail in Table A2 in the Appendix. Bayesian Information Criterion (short: BIC; criterion for model selection, [SINHA ET AL. \(2021\)](#)); Akaike Information Criterion (short: AIC; criterion comparing statistical models balancing model fit and model complexity, [SINHA ET AL. \(2021\)](#)), entropy (measure of dispersion in a probability mass function); class size (share of cells within one latent class must not be below 10 %); precision of class affiliation (measures the probability with which a single cell is assigned to a latent class) and logical fit (Logical fit of the composition of latent classes). In the Supplementary Material (Tables A3 to A5) all fit indices' results are listed.

Model fit was given by BIC and AIC (lower values indicate more accurate model fits) and an entropy above or close to 0.8 (ranging from 0 to 1) ([Sinha et al., 2021](#); [Weller et al., 2020](#)). Also, smallest class size (min of 10 %) was used to further determine the LC model ([Sinha et al., 2021](#)). An LCA was conducted for each of the three municipalities using the default function provided by poLCA in R ([Linzer and Lewis, 2013](#)). The expected outcome of the LCA consists of one dataset per municipality, in which each 100 m × 100 m grid cell is associated with probabilities of assignment to the respective classes. Furthermore, kernel density has been used to display the spatial distribution of the resulting LCs within the model cities.

2.3. HRI

An HRI was established following the risk triangle approach of [Crichton \(1999\)](#) used frequently in heat risk related studies and recommended by the IPCC (e.g., [Buscail et al., 2012](#); [Chen et al., 2018](#); [Dong et al., 2020](#)), defined as follows:

$$\text{Heat Risk} = \text{Hazard Index} + \text{Exposure Index} + \text{Sensitivity Index}$$

HAZARD is represented by satellite-based data on Land Surface Temperature (LST) obtained from the Landsat mission, featuring a high spatial resolution of 100 m with a revisit time of 16 days. For this work, Level 2 Collection 2 thermal imagery from Landsat 8 and 9 ([EROS, 2020](#)) was prepared for the time period 2013–2024 in order to compensate data inconsistencies and gaps due to revisit time, cloud cover, and different acquisition orbits. A total of 972, 608, and 624 single acquisitions were prepared for the cities of Augsburg, Hamm, and Zwickau respectively. For the analysis, clouds were masked from every single acquisition and statistical aggregates in terms of the annual mean LST were computed for each city ([Leichtle et al., 2023a](#)). The LST data depict the long-term annual mean temperature patterns within each cell of the 100 m × 100 m grid. To implement these data in the HRI (hazard component), quantiles have been used to group the LST data in five groups with the highest value of 5 depicting the warmest 20 % of grid cells and the lowest value of 1 depicting the coolest 20 % of grid cells. While LST does not allow for direct assumptions about heat risk, it is commonly employed as a robust proxy to map spatial patterns of urban heat (e.g. [Zhang et al., 2025](#)).

EXPOSURE is depicted by the number of inhabitants potentially exposed to heat stress and thus describes the population share which is potentially affected by the hazard ([Leichtle et al., 2023b](#)). To calculate the exposure in this study the number of inhabitants within each 100 m × 100 m grid cell was approximated using the 2022 census data (see: [German Federal Statistics Office, 2024b](#)). In accordance with the hazard component the exposure component was categorized into five groups with the lowest value of 1 depicting the least populated 20 % of grid cells. Higher exposure is represented by higher index points.

SENSITIVITY is defined as the individual vulnerability to heat-related health problems. In this study, it is represented by net rent ([Kenny et al., 2010](#)), reflecting inhabitants' financial capability to adapt to heat (i.e. purchasing cooling devices or paying entry fees to public swimming pools); age (> 65 and < 10) ([Cheng et al., 2018](#); [Ebi et al., 2021](#); [Seebaß, 2017](#)); household size ([Hass and Ellis, 2019](#))

and share of foreign population (here birthplace \neq Germany) which may indicate potential challenges in individual adaptation processes due to cultural and language barriers (Ebi et al., 2021). Due to data availability, additional influencing factors on heat-related health problems such as medical information including chronic illness (Kenny et al., 2010) could not be considered. As mentioned before all continuous sensitivity indicators have been categorized into three categories (below average, average, above average) which could furthermore also be described as low, average or high indication for heat sensitivity. The value 1 was assigned to the lowest associated heat sensitivity while 2 represented values indicating a medium and 3 a high heat sensitivity regarding each sensitivity indicator. For instance, above average net rent was associated with low heat sensitivity due to the assumption of individual's higher financial capital while an above average amount of individuals aged 65 or older was associated with higher heat sensitivity in a

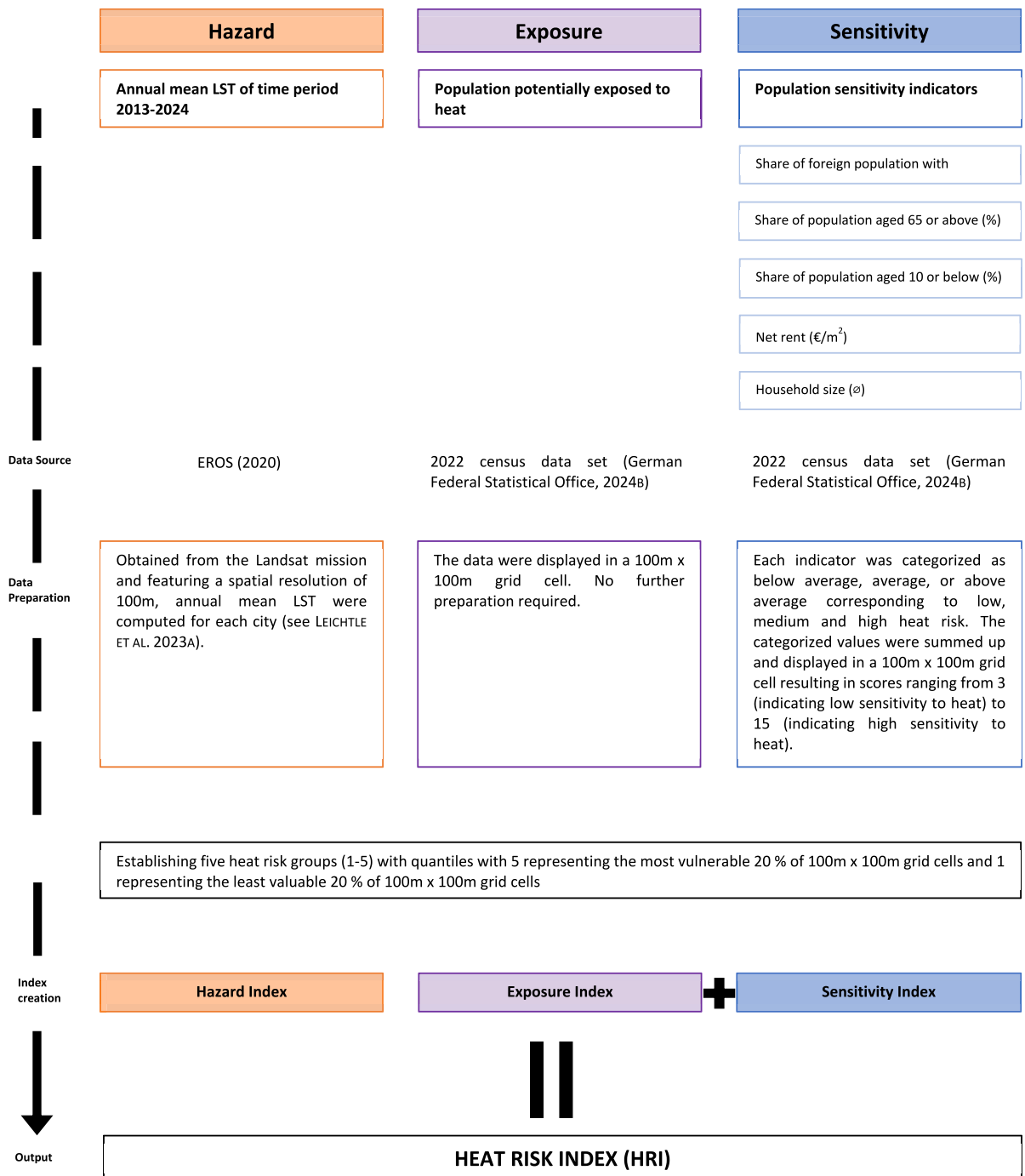


Fig. 1. Illustration of HRI construction process.

100 m × 100 m grid cell. Values for all indicators were summed up to a potential maximum of 15 points per grid cell. No weighting was applied between the sensitivity indicators. To ensure equal weighting among the hazard index, exposure index and sensitivity index, the 15-point scoring system was condensed to a 5-point scoring system.

Finally, an HRI was calculated. Each 100 m × 100 m grid cell can reach a maximum of 15 HRI points (5 points for hazard, exposure and sensitivity each). An equal weights approach was chosen as there is no consensus about weighting HRIs in the scientific community (Chen et al., 2018). Additive HRI approaches have been used widely in the current scientific literature (e.g. Birkmann et al., 2022; Xiang et al., 2022). However, equal weights among hazard, exposure and sensitivity are often used in HRI construction (e.g., Hu et al., 2017; Mitchell and Chakraborty, 2015). Fig. 1 illustrates the HRI construction process in this study.

A higher HRI displays a higher risk for heat stress for individuals living or spending time in the area. This approach was chosen in order to provide a manageable, clear and easy-to-use HRI for stakeholders from various disciplines. Fig. A2 in the Supplementary Material clarifies the data processing.

3. Results

3.1. Identification of heat-health-related population groups

For each city a distinct LCA was conducted containing a different amount of complete data sets due to data availability and city size (Fig. 2).

Typically, LCA is more accurate with a higher number of available datasets as small groups might be overseen in small datasets. Sinha et al. (2021) suggests a minimum of $n = 300$ for LCA which was met in all three cities (Fig. 1). Spatial variability in data availability in all three model cities – outskirts are less well represented than centres - might lead to overlooking high vulnerability spots. However, within the city centre all three model cities show a spatially comprehensive data availability.

In all LCA runs, a maximum of 5 classes for all three municipalities was detected. BIC, AIC, entropy and class size were used to narrow down potential model fits. To select the LCA model finally used for further analysis precision of class affiliation was used as decisive criterion to determine the final model for each city, as a more precise fit also entails a higher planning security for municipal stakeholders. For Augsburg and Zwickau, the LC model with three LCs was determined as the best fit model respectively. However, for Hamm the model with four LCs showed a slightly better fit than the model with three LCs in the initial fit indices. In regard to comparability between the cities, three latent classes for each model city were chosen.

For Augsburg, three LCs could be established (Table 2). Class one (Augsburg 1) is characterized by grid cells being home to either an average or higher share of foreign population, with a higher population density, an average household size of 2 to 3 individuals, an average net rent regarding the city's rent index, a high share of individuals aged 10 or younger as well as a low share of elderly individuals. Class two (Augsburg 2) in contrast is characterized by a low or average share of foreign population, average or high number of inhabitants, a higher possibility for individuals to live in multi-person households (> 3 persons), a higher than average or average net rent, a low share of individuals aged 10 or younger as well as a high or average share of individuals aged 65 or older. Finally, class three (Augsburg 3) is defined by an average or low share of foreign population, comparatively low number of inhabitants, a higher share of single-person-households, a low or average net rent, a low share of children younger than 10 as well as an average or high share of elderly individuals.

The second LCA identified three LCs for Hamm (Table 3) with class one (Hamm 1) being classified by an average share of foreign population, a low or average population density, a high number of single-person households, a low or average net rent compared to the city's rent index as well as an average share of individuals aged 10 or younger or 65 or older respectively. Class two (Hamm 2) displays an average or high share of foreign population, a high population density, smaller households and an average net rent. In addition, a high share of individuals aged 10 or younger is likely while the share of individuals aged 65 or older is lower than average. Finally, class three (Hamm 3) is defined by a low or average share of foreign population, an average population density, a higher share of multi-person households, average net rents, a low share of individuals aged 10 or younger as well as a high share of individuals aged 65 or older.

In Zwickau three LCs were also identified (Table 4) with class one (Zwickau 1) being characterized by a high share of foreign

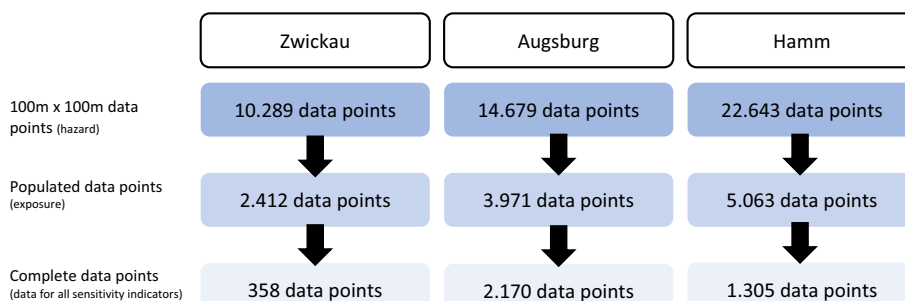


Fig. 2. Flow chart showing data point availability for LCA for each city. Number of datasets used for the LCA per city.

Table 2

Latent class characteristics of identified LCs in Augsburg. (–: below average, 0: average, +: above average). Colours indicating overall classes.

Indicator	Augsburg 1 (OC1)	Augsburg 2 (OC2)	Augsburg 3 (OC3)
Share of foreign population	0/+	–/0	–/0
Inhabitants	+	0/+	–
Size of households	0	0/+	–/0
Net rent	0	0/+	–/0
Aged 10 or younger	+	–	–
Aged 65 or older	–	0/+	0/+

Table 3

Latent class characteristics of identified LCs in Hamm. (–: below average, 0: average, +: above average). Colours indicating overall classes.

Indicator	Hamm 1 (OC1)	Hamm 2 (OC1)	Hamm 3 (OC2)
Share of foreign population	0	0/+	–/0
Inhabitants	–/0	+	0
Size of households	–	–/0	0/+
Net rent	–/0	0	0
Aged 10 or younger	0	+	–
Aged 65 or older	0	–	+

Table 4

Latent class characteristics of identified LCs in Zwickau. (–: below average, 0: average, +: above average). Colours indicating overall classes.

Indicator	Zwickau 1 (OC1)	Zwickau 2 (OC3)	Zwickau 3 (OC2)
Share of foreign population	+	–	0/+
Inhabitants	0/+	0/+	0/+
Size of households	0	–	0/+
Net rent	0	0	0
Aged 10 or younger	+	–	–
Aged 65 or older	–	+	–/0/+

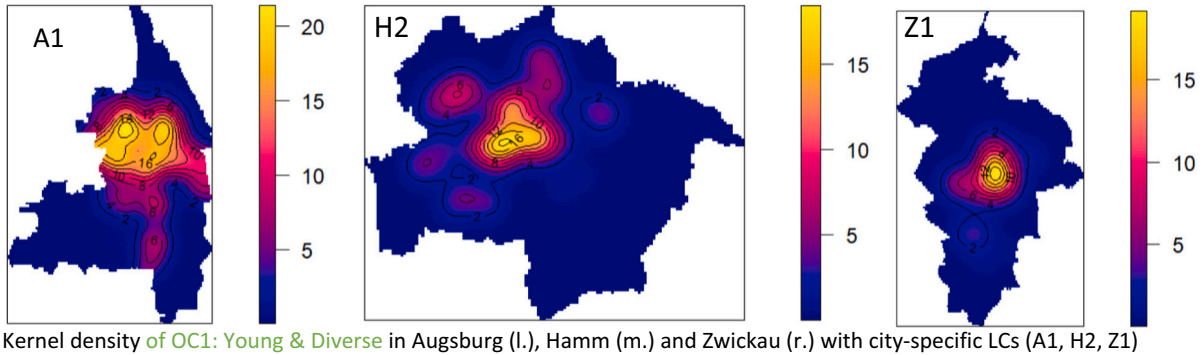
population, an average or high population density, 2 to 3-person households, an average net rent, a high share of individuals aged 10 or younger as well as a low share of elderly individuals. Class two (Zwickau 2) features a low share of foreign population, an average or high population density, a high share of single-person households, an average net rent as well as a low share of individuals aged 10 or younger and a high share of individuals aged 65 or older. Finally, class three (Zwickau 3) is characterized by an average or high share of foreign population, an average or high population density, a household size of 2 to 3-persons or more, an average net rent, a low share of children younger than 10 years as well as varying shares of elderly individuals.

By comparing the three LCs identified for each model city (A1 to A3, H1 to H3, Z1 to Z3), three overall classes (OC1: A1, H2, Z1, OC2: A2, H3, Z3, OC3: A3, H1, Z2) could be established. While A1, H2 and Z1 and respectively A2, H3, and Z3, show very similar characteristics and thus could be easily grouped to OC1 and OC2 respectively, OC3 is not as sharply defined with A3, H1 and Z2 showing more differences (Tables 2–4).

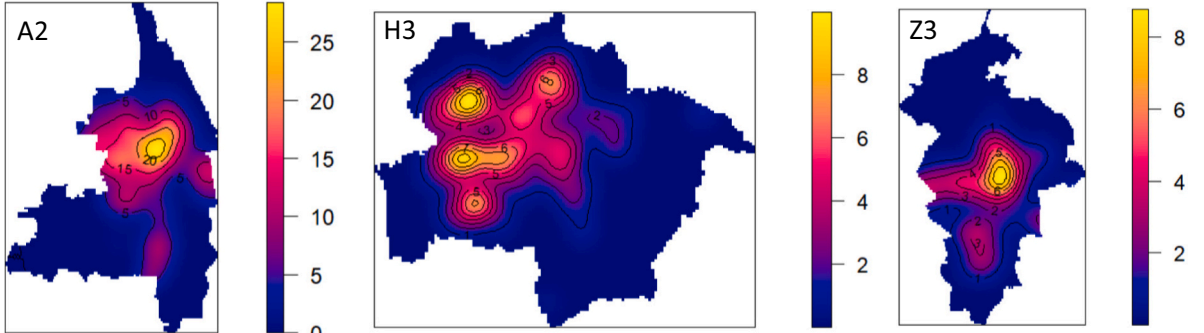
The 100 m × 100 m grid cells assigned to the first overall class (OC1) are characterized by an average or above average share of foreign population, an above average number of inhabitants, an average household size of 2 to 3 individuals, average net rent, an above average share of children aged 10 or younger and a below average share of adults above or at the age of 65. OC1 therefore is referred to as “Young & Diverse”.

The second overall class (OC2) is characterized by an average or below average share of foreign population (divergent for Zwickau, which shows all possible expressions), 2 to 3 individuals per household with a high share of single-households in Hamm, an average net rent, below average share of children aged 10 or younger and all possible expressions for the share of individuals at or above the age of 65. OC2 therefore is referred to as “Adults & Citizen”. The third overall class (OC3) shows more differences in class traits between the model cities. The share of foreign population is below average or average within the class three tiles. Additionally, the household size is below average for all three cities, indicating a high share of single person households. The share of individuals aged 65 and older is average or above average for all model cities. For Augsburg tiles in class three are more likely to have a below average population density, while the tiles in Hamm show a below average or average population density and tiles in Zwickau show an average or above average population density. Finally, the number of individuals younger than or aged 10 is below average for Augsburg and Zwickau but average in Hamm. OC3 is characterized by “Elderly & Single-Household”.

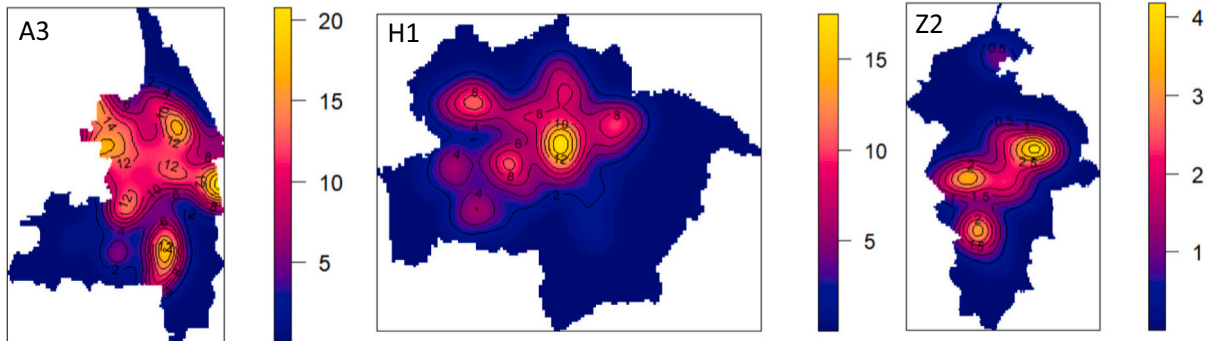
A kernel density analysis was conducted to identify possible spatial clusters of population groups within each city. Identifying such clusters is highly important for implementing heat adaptation and mitigation measures in urban planning as preferentially addressing certain population groups is possible via focusing on certain city areas. For instance, OC1 “Young & Diverse” forms one distinct cluster in the city centres of each municipality. In Augsburg the “Young & Diverse” can also be found in the city's north, the city quarter of “Oberhausen” (Fig. 3). “Adults & Citizens” is either mainly found in city quarters outside the inner city, such as in Hamm where “Adults



Kernel density of OC1: Young & Diverse in Augsburg (l.), Hamm (m.) and Zwickau (r.) with city-specific LCs (A1, H2, Z1)



Kernel density of OC2: Adults & Citizens in Augsburg (l.), Hamm (m.) and Zwickau (r.) with city-specific LCs (A2, H3, Z3)



Kernel density of OC3: Elderly & Single-Household in Augsburg (l.), Hamm (m.) and Zwickau (r.) with city-specific LCs (A3, H1, Z2)

Fig. 3. Kernel density of all three overall classes. Upper row: OC1, middle row: OC2, lowest row: OC3, Augsburg (l.), Hamm (m.), Zwickau (r.). Base maps of each city are found in the Supplementary Material (Figs. A3a, A3b and A3c).

“& Citizens” is located mainly in the western part of the city. In Augsburg and Zwickau “Adults & Citizens” is distributed in the city centre (though for Augsburg not in the city quarter of “Oberhausen”) and within neighbouring areas (Fig. 3).

And, “Elderly & Single-Household” is spread all over the city in Augsburg, where several “Elderly & Single-Household” hotspots appear. For Hamm, one “Elderly & Single-Household” hotspot is found in the eastern part of the city with multiple smaller hotspots spread over all city quarters. In Zwickau, there are multiple “Elderly & Single-Household” hotspots with less “Elderly & Single-Household” tiles found in the city centre (Fig. 3).

3.2. Hazard, exposure, and sensitivity maps

Before calculating an HRI composed of hazard, exposure and sensitivity, maps for each model city depicting the risk components were derived. The hazard maps show the LST in each model city. Comparable LST-Ranges appear in the three cities with the minimum value of 23.6 °C (Hamm) and the maximum value of 36.4 °C (Augsburg). In all study sites LST tends to be higher in the city centre or areas with a densely built environment. The lowest LST values can be found in the city outskirts (Fig. 4).



Fig. 4. Hazard Maps of Augsburg (l.), Hamm (m.), Zwickau (r.) in a $100\text{ m} \times 100\text{ m}$ resolution based on LST data (data source: [EROS, 2020](#)). Lower numbers indicate lower risk of hazard.

The number of de facto inhabitants was used as an indicator for heat exposure in this study. In all three model cities the city centre contains high exposure spots. However, there are also always spots of high exposure in most of the other city quarters, often also located in areas within the city outskirts. In addition, there are city quarters with a generally low exposure found within all three cities (Fig. 5).

Heat sensitivity was estimated by using sociodemographic data retrieved from the 2022 census. The heat sensitivity index in this study is composed of the following indicators: age (10 years or younger or 65 years or older respectively), net rent, household size and share of foreign population (Fig. 6).

Rural-oriented neighbourhoods, typically with a higher share of single-family homes, a higher number of inhabitants per household as well as high-income city quarters are mainly characterized by low sensitivity spots (e.g., city quarters within Augsburg: Göggingen, Haunstetten (Fig. 6a); Hamm: Rhynern, Uentrop, (Fig. 6b)). For Zwickau, lower sensitivity index values are found in the outskirts of Zwickau, especially in the south-western city quarters (Fig. 6c). However, in all three cities, low sensitivity index values are not



Fig. 5. Exposure Maps of Augsburg (a), Hamm (b) and Zwickau (c) in a $100\text{ m} \times 100\text{ m}$ resolution based on inhabitant census 2022 data (Source: [German Federal Statistics Office, 2024b](#)). Lighter purple indicates a lower exposure, darker purple indicates a high exposure. (For interpretation of the references to colour in this figure legend, the reader is referred to the web version of this article.)

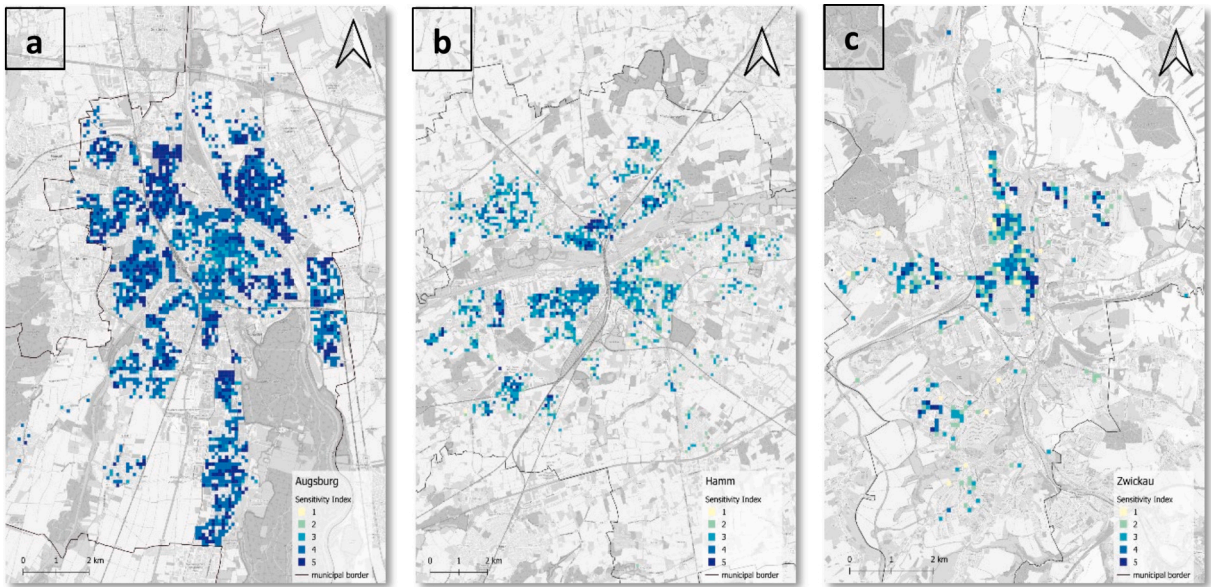


Fig. 6. Sensitivity Maps of Augsburg (a), Hamm (b) and Zwickau (c) in a $100 \text{ m} \times 100 \text{ m}$ resolution based on census data (net rent, age > 65 , age < 10 , household size, share of foreign population) depicting social vulnerability related to heat risk. Light blue indicating lower sensitivity, dark blue indicated higher sensitivity. (For interpretation of the references to colour in this figure legend, the reader is referred to the web version of this article.)

exclusively found in areas with the characteristics mentioned earlier, but also found scattered throughout the city area. High sensitivity spots are likely to be found in densely-populated city quarters. Also, it is noticeable that sensitivity spots are overrepresented in structurally weaker but urban-oriented areas when comparing the spatial heat sensitivity index results with a social space analysis conducted by the three municipalities (Kiefer and Bachmeir, 2017; German Federal Ministry For Housing, Urban Development And Building, 2017; Ministry of Internal Affairs, 2022) (e.g., city quarters within Augsburg: Oberhausen, around Wertachbrücke and along Donauwörtherstraße (Fig. 6a), Hamm: north of the river Lippe area Schottschleife (Fig. 6b), Zwickau: Eckersbach (Fig. 6c)). Furthermore, city quarters with a high share of single-households in densely-populated areas are often but not only found in the city centres and show higher heat sensitivity index values. In the north of Hamm areas with a high share of children aged 10 or younger was

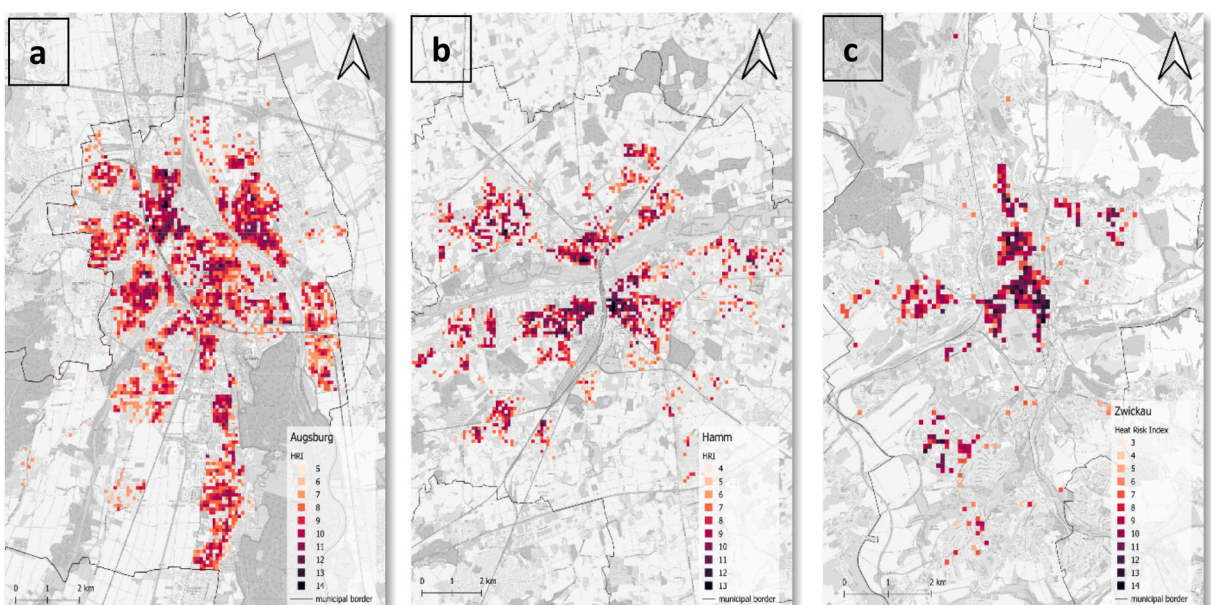


Fig. 7. Heat Risk Maps of Augsburg (a), Hamm (b) and Zwickau (c) in a $100 \text{ m} \times 100 \text{ m}$ resolution based on inhabitant census data (data source: German Federal Statistics Office (2024b)). Lower HRI values indicating lower heat risk. HRI composed of hazard, exposure and sensitivity.

found to show a higher amount of heat sensitivity spots.

3.3. Heat risk index/heat risk maps

An HRI was established analogously for each model city (methodological approach). At a glance a comprehensible spatial variation of heat risk is visible within each city. Even though the absolute range of the HRI values differ slightly between the model cities (Augsburg: 5 to 14; Hamm: 4 to 13; Zwickau: 3 to 14), the highest HRI values are generally found in the city centres respectively while the lowest heat risk values are mainly found in the outskirts often being surrounded by green spaces. In Hamm and Augsburg there are high heat risk spots found in different city quarters while in Zwickau all high heat risk spots are located in the city centre (Fig. 7). This might be caused by a polycentric city structure in Augsburg and Hamm opposed to a monocentric city structure in Zwickau. Even though, absolute HRI values are not directly comparable, similar HRI patterns can be found in all three cities.

Areas with detached houses, higher net rents, and rural characteristics (e.g., city quarters within Augsburg: Göggingen, Spickel-Herrenbach) exhibit the lowest heat risk values. Also, often a high share of elderly residents and a below average population density is found in these areas. Often these areas were located in the outer city quarters. Furthermore, areas in proximity to blue infrastructure (Augsburg: around rivers Lech, Wertach and Fabrikkanal) as well as in near proximity to green infrastructure (e.g., Hamm: Südfriedhof, Ahseteich) show lower HRI values. However, city quarters might contain areas with very high and very low HRI values located in near proximity to each other. The highest HRI values are found in socially deprived neighbourhoods (e.g., city quarters within Augsburg: parts of Oberhausen, Hamm: Schottschleife), areas with a densely built-environment such as the city centre, areas with single-households in multi-apartment buildings and areas with limited green spaces such as arterial roads and high-traffic areas.

In all three cities some especially vulnerable institutions such as nursing homes or kindergartens as well as medical facilities can be found within high heat risk areas. Those are often located in socially deprived areas, areas with a densely built environment or densely-populated areas especially with a high share of multi-family buildings and single-households. Furthermore, areas and city quarters being shaped by rural structures with a loose built infrastructure and many green spaces, areas being in near proximity to blue infrastructure, areas with a high share of inhabitants with a high-income (often paired with a high share of elderly inhabitants) show lower HRI values. Often residential areas show higher HRI values than industrial areas or areas with a high share of recreational facilities. Highest HRI values often are reached when areas possess more than one of the above-mentioned characteristics. However, typically high heat risk areas also contained low heat risk spots, typically in proximity to blue or green infrastructure.

3.4. Latent classes and heat risk

In order to design heat risk mitigation and adaptation strategies for a municipality, locating heat risk patterns as well as patterns of population structure might be helpful. In the following, these patterns for Augsburg, Hamm and Zwickau are presented (Fig. 8).

A relation between HRI values and latent class affiliation of the 100 m × 100 m grid cells has been observed. In all three cities, grid cells assigned to latent class OC1 (Young & Diverse, Augsburg 1, Hamm 2, Zwickau 1) show also the highest HRI values. In Augsburg OC1-areas are spread over the city area with visible hotspots in central city quarters (e.g., University Quarter, Oberhausen, Lechhausen). This observation is also true for Hamm, where OC1-areas are mainly found around the main station within the city centre and Zwickau (e.g., Marienthal, city centre). The OC3 (Augsburg 3, Hamm 1, Zwickau 2) is found to have the lowest HRI values in Augsburg and Hamm being located mainly in the outskirts of the cities (e.g., Augsburg: Hochzoll, Haunstetten, Göggingen, northern Lechhausen). Deviating from that in Zwickau grid cells classified as OC2 shows the lowest HRI values. However, in Zwickau OC3 is a very small class with few data sets whilst OC2 has a wide range of HRI values. OC3 shows characteristics of an in-between class with a wide range of HRI points being an indicator for a more heterogenous indicating that OC3 is a more city specific class. Thus, areas with these characteristics are found in clusters as well as isolated throughout each city area.

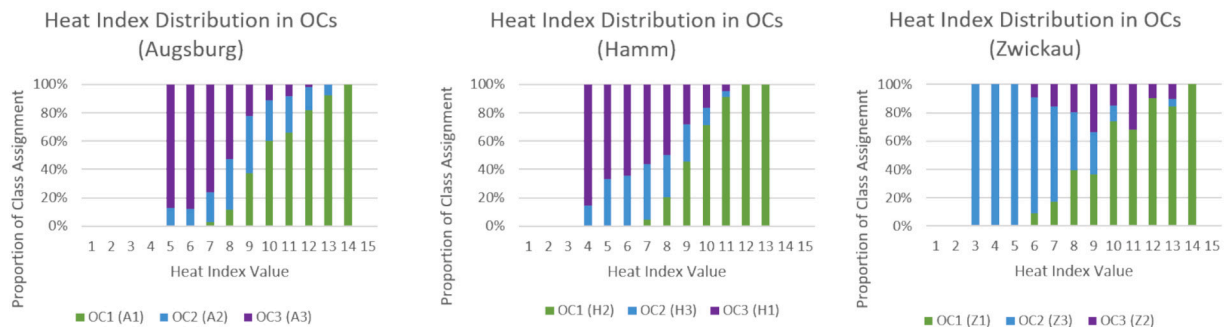


Fig. 8. Heat Index Distribution in OCs per city with Augsburg (upper left), Hamm (upper right) and Zwickau (lower right) and OC1 (green), OC2 (blue), OC3 (purple). (For interpretation of the references to colour in this figure legend, the reader is referred to the web version of this article.)

4. Discussion

HRIs provide information to locate areas with high heat risk. Recently, establishing HRIs for urban environments has been highly discussed in scientific literature (e.g. [Jay et al., 2021](#); [Mohammed, 2025](#)). Also, many scholars emphasize the need for heat risk management on a community scale (e.g. [Cui et al., 2024](#); [Guardaro et al., 2022](#)) with HRIs supporting local stakeholders in short and long-term planning processes (e.g. [Jay et al., 2021](#); [Roberts et al., 2025](#)) by providing information not only on heat risk determined by solely climatological but also sociodemographic vulnerability (e.g. [Ho et al., 2025](#); [Hass and Ellis, 2019](#); [Mohammed, 2025](#)). Overlooking socio-demographic factors in establishing HRIs can negatively influence the allocation of priorities in heat risk management ([Mohammed, 2025](#)) and lead to the exclusion of highly vulnerable populations from adequate protection measures. In this study, an HRI was developed for three German cities at a fine spatial resolution of 100 m × 100 m grid, a level of detail that allows for precise identification of vulnerable areas. The HRI integrates hazard, exposure, and sensitivity, with the latter capturing indicators of social vulnerability. This approach relies solely on open-source data as well as tools to ease accessibility and reproducibility of the approach for other municipalities within Germany. By studying hazard, exposure and sensitivity indexes, planners can access information on where the highest physical strain of heat can be found (hazard), where the most individuals are exposed to weather (exposure) and where especially vulnerable individuals are located (sensitivity). This aligns with HRI construction in many papers of the current literature (e.g. [Buscail et al., 2012](#); [Ellena et al., 2023](#); [Pappalardo et al., 2023](#)).

In practice, sensitivity often seems the aspect which can be changed the fastest and easiest with individual adaptation it might also be the most difficult to achieve for vulnerable population groups ([Friesenecker et al., 2025](#)). Mitigating the hazard component might entail large infrastructural changes or reaching the 1.5 °C goal stated in the Paris Agreement in order to achieve a noticeable cooling in specific areas. Infrastructural changes which entail a significant influence on thermal comfort are often related to high monetary and time expenses ([Kumar et al., 2024](#)). Mitigating the exposure index (i.e. through relocation of inhabitants) is hardly feasible in practice, altering the sensitivity index often seems to be the most practicable and realistic approach for a quick fix in a municipalities heat risk management. While many HRIs in the current literature already implement social vulnerability via a sensitivity index (e.g. [Ellena et al., 2023](#); [Mohammed, 2025](#); [Roberts et al., 2025](#)) and thus offer insights into the location of heat risk, this study adds information on the factors contributing to heat vulnerability at the grid-cell level. Accordingly, using LCA, three LCs were derived for each city to characterize population patterns with respect to socio-demographic structures. The characteristics of these LCs were similar across cities, allowing for the establishment of overall classes. By implementing LCA within the HRI approach in this study, clusters of vulnerable groups in high heat risk areas can be identified for the three model cities, enhancing the visibility of planning priorities. This information supports city planners in developing targeted adaptation and mitigation strategies for heterogeneous populations. Also, in further steps, this approach allows the development of personas, and thus supporting local stakeholders implementing target-group oriented heat risk mitigation and adaptation strategies potentially improving the efficacy of heat risk mitigation and adaptation measures on a city-level. Additionally, follow up research on how local stakeholders implemented the study's results in their heat risk management might be relevant for future research.

The here established HRI allows policy makers to easily locate the overall highest heat risk areas within each model city. Unsurprisingly the highest HRI values are found in the city centres while the lowest ones are located in the city outskirts typically situated in proximity to wide green spaces (see Chapter 3.3). Also, differences occur in the mono- vs. polycentric city structures of the model cities, leaving hot spots in Zwickau being located within one area while Augsburg and Hamm show multiple hot spot areas. Despite the fact that absolute HRI values are not directly comparable, similar spatial patterns are observed in all three cities, as might be expected. Additionally, this study offers an approach for policymakers to identify not only high heat risk hotspots but also the populations residing in these areas, enabling targeted and effective heat risk management. This information benefits heat risk management as follows:

Social capital, a complex construct including trust, interpersonal relationships, and reciprocity, plays a crucial role, in individual heat risk adaptation strategies ([Ho et al., 2025](#); [Hass and Ellis, 2019](#)) and thus, enhances adaptation to disasters. Areas with clusters of OC3 (Elderly & Single-Household) could particularly benefit from strategies that promote social capital, such as voluntary neighbourhood support, heat-alert phone calls, or providing cool communal spaces. These interventions not only offer direct assistance during heat waves but also strengthen social networks, enabling individuals to exchange experiences, access resources, and support one another in adaptation efforts as a study by [Guardaro et al. \(2022\)](#) underlines. Rising awareness is an important factor for strengthening individual heat risk adaptation, as many individuals are unaware of their personal risk ([Howe and Leiserowitz, 2013](#)). Educating individuals on their personal heat risk vulnerability and discussing factors such as living area, chronic illnesses or age and providing additional information such as heat risk maps ([Ho et al., 2025](#)), organizing target-group-oriented city walks to help individuals find cool spots and routes can enhance individuals' heat adaptation behaviour. Finally, using multiple communication channels (e.g. social media, religious communities, flyers, local newspapers, etc.) as well as providing accessible and multilingual information ensures that guidance reaches diverse populations and supports effective heat risk management. For instance, areas with clusters of OC1 (Young & Diverse) might benefit most of these measures as they are not immediately recognized as vulnerable and more important often do not perceive themselves as such. *Infrastructural changes*, such as redesigning green areas, playgrounds, and public spaces, as well as providing shaded seating and drinking fountains, can help individuals find cool places during hot days and might make public places more accessible during heat events (e.g., [Jay et al., 2021](#); [Kumar et al., 2024](#); [Park et al., 2022](#)). For instance, inhabitants of areas classified as OC1 (Young & Diverse) as well as OC3 (Elderly & Single Household) might benefit most from infrastructural changes as they are more likely to be limited in their personal adaptation capacity and tend to spend more time in the near proximity to their home. However, OC1 (Young & Diverse) is mainly found in densely-built areas such as the city centres of each of the model cities. Thus, redesigning existing infrastructure such as incorporating vertical or rooftop greening (e. g., [Sadeghi et al.,](#)

2022; Susca et al., 2022), shading elements (e. g., Kántor et al., 2018), establishing pocket parks (e. g., Park et al., 2022) as well as setting up cooling centres within the existing infrastructure in high risk areas might help reducing heat risk for OC1 (Young & Diverse) more effectively. Increasing the usability and redesigning existing green infrastructure, might also support the adaptive capacity of OC1. Thus, adapting green spaces and playgrounds to the needs of OC1 encourages usage and supports stress-free daily activities, while cooling interventions in OC3 areas improve accessibility and comfort for less mobile populations. Overall, tailored infrastructural adaptations reduce heat exposure and support adaptive behaviours across diverse urban populations.

As mentioned in Chapter 3.4 a relationship between HRI values and LC affiliation of the 100 m × 100 m grid cells has been observed. OC1 (Young & Diverse) corresponds to the highest HRI values, whereas OC3 (Elderly & Single-Household) shows the lowest, with OC2 (Adults & Citizen) positioned in between. While these insights already assist local stakeholders and policymakers in prioritizing short- and long-term heat mitigation and adaptation strategies, hidden hotspots within each OC group may still be overlooked. As heat risk management is often constrained by factors such as financial and human resources or time, municipalities could benefit from identifying heat vulnerability hotspots across different population groups to address urban heat risk comprehensively as well as efficiently. When highlighting the most vulnerable 1 % of each OC group in each city, heat risk hotspots emerge that are not captured by the general HRI and thus, offer new perspectives for policy makers. Although the overall HRI primarily identifies high heat risk areas in the city centres, this pattern applies only to the most vulnerable 1 % of OC1 (Young & Diverse), where the highest HRI values are concentrated. In contrast, the most vulnerable areas within OC2 (Adults & Citizen) and OC3 (Elderly & Single-Household) are more scattered across the city. Especially OC3 (Elderly & Single-Household) is found in the city outskirts as for instance in the outer districts of the model city Hamm. Specifically, the districts of Rhynern, Berge, and Werries in the north-eastern and south-eastern parts of Hamm exhibit low to medium hazard index values (see Fig. 4) as well as low to medium exposure index values (see Fig. 5). However, in the district Werries a cluster of five spatially coherent 100 m × 100 m grid cells belonging to the most vulnerable 1 % of OC3 (Elderly & Single-Household) can be identified. In addition, isolated grid cells of the most vulnerable 1 % of OC3 (Elderly & Single-Household) are detected in other urban fringe districts across all three model cities. These areas might have been not identified as high risk by a traditional HRI approach. These information and evaluation options gathered from this study's methodological approach can make valuable contributions to local heat risk management. Finally, the inclusion of sensitivity, especially when linking it with the OCs established through LCA within the HRI framework in this study enables the identification of the most vulnerable groups rather than merely the hottest locations. Thereby supporting more equitable and targeted heat adaptation measures that contribute to addressing climate injustice in disaster risk or rather heat risk management as also suggested by other scholars (e.g. Pappalardo et al., 2023).

One limiting aspect of many HRIs is limited data availability (e.g., influencing choice of indicators, scale of data, lack of socio-economic data, etc.) and data accuracy (e.g., undiagnosed health issues, incomplete datasets, etc.). This is especially true when operating on a high spatial resolution such as within this study. Changes in individual characteristics (such as age, chronological illnesses, or financial and social status) can rapidly alter an area's class affiliation, and socioeconomic data often only provide a temporary snapshot making HRI assessments sensitive to short-term demographic shifts which is also true for the census data used within this study. Additionally, changes in the built environment might change LST estimation over time while migration processes alter exposure. Often, the *de facto* and *de jure* population of an area show different characteristics and thus different heat-related health risks (e.g., Buscail et al., 2012; Buzási, 2022; Dumont and Mathis, 2023; Ellena et al., 2023). This is also true for data in LCA which is dependent on the input data and often is based on temporal, subjective information. However, in Germany census data is retrieved regularly and thus could be updated easily following our HRI approach. Another aspect is that all information was given by inhabitants themselves during the census 2022 survey (e.g., Kácha et al., 2022; Nguyen et al., 2024). Data availability often limits the indicators included in LCA (Keller et al., 2024; Korkala et al., 2014; Nguyen et al., 2024), which was also the case in this study as there is no nationwide open-source data regarding chronological illnesses in Germany.

The assumption that individuals within a certain area (e.g., city quarter etc.) are a homogenous group of individuals might lead to data inaccuracy and distortion (e.g., Forceville et al., 2024; Hammer et al., 2020; Klopfer and Pfeiffer, 2023; Pappalardo et al., 2023). Also, LCA results in class affiliation probabilities meaning that a proper class assignment cannot be guaranteed (Kácha et al., 2022; Weller et al., 2020). This also entails that an exact number of class size, percentage of tiles being assigned to one class or a secure class affiliation is impossible. Assigned tiles might not show all characteristics defining one group. For instance, an area being assigned the OC1 class might show a high number of young children, a high share of foreign population but can – unlike its class description – also be home to many individuals aged 65 or above. To limit misidentification this study used various fit statistics (see Supplementary Material Table A3-A5) including entropy and latent class size. On the one hand, assigning class names eases the discourse about classes, especially with stakeholders involved in planning, on the other hand it entails the risk of deception as simplified and catchy names mostly cannot represent complex classes (Kácha et al., 2022; Weller et al., 2020) which also might be deceptive or confusing for local planning stakeholders in charge. Furthermore, various steps in LCA are dependent on the researchers' subjective decisions such as which data and participants to include within the study (Korkala et al., 2014), how the data is prepared for LCA (Liao et al., 2024), which indicators and model fits are chosen for the final class assignment or how the final classes are interpreted (Kácha et al., 2022).

Also, the design of HRIs often entails a lot of subjective decisions made by the researcher team (e.g. indicator decision, weighting approach) (Hammer et al., 2020). The open-source approach within this study made a trade-off between simplification and accessibility on the one hand and accuracy on the other hand. While heat hazards cannot solely be determined by LST but entail a complex set of indicators such as humidity, air flow and air temperature, incorporating a huge set of indicators might be less accessible and reduce the approaches' transferability to other municipalities. However, various scholars state, that LST can reflect the spatial distribution of urban heat (e.g. Cheng et al., 2021; Zhang et al., 2025). This study used annual mean LST, which may dampen extreme summer heat signals and potentially underrepresent acute hotspots, although sensitivity checks using summer mean LST showed only marginal

differences in the resulting LST patterns. Moreover, uncertainty within the HRI results is caused by the lack of a standard weighting known to be most accurate in regard to balancing the HRI between hazard, exposure and sensitivity. Therefore, in this study equal weighting between indexes, might not depict reality accurately. This leads to more insecure and less comparable HRI results (e.g., [Chen et al., 2018](#); [Hua et al., 2021](#)). Additionally, weighting within each index (in our study between sensitivity indicators) raises similar insecurities.

Finally, this study was constructed in the context of German municipalities. However, the socio-demographic data used within this study is only available in this specific resolution within Germany, some of these data might vary significantly across countries or might not be available at all. Additionally, Germany has relatively robust census data which might not be true for different countries. Especially, for regions located in the global south with different data availability and accuracy as well as different key factors for vulnerability (e.g. due to cultural differences, higher share of outdoor and agricultural workers and dependencies) (e.g. [Adjei et al., 2025](#)) the approach presented within this study might need to be adapted accordingly.

Implementing LCA in the development of an HRI for Augsburg, Hamm, and Zwickau helped identify different groups of inhabitants living within high heat risk areas and provided evaluation options for local stakeholders and policymakers to detect hidden hotspots across different OC groups. Building on these findings, several directions for future research can further improve the accuracy, development, application, and generalizability of HRIs. One area of interest concerns the generalizability of population classes. Whether similar classes can be identified not only in these three municipalities but across multiple German cities is a question for future research. Identifying population structures and heat risk patterns that are generally valid for many cities could greatly simplify heat risk management and reduce the steps needed to create HRIs. Another important research field involves exploring alternative classification approaches. Comparing the advantages and limitations of LCA with other classification methods, such as k-means clustering for socioeconomic data, could provide valuable insights in HRI construction. Also, examining the question whether inter-group relationships are found between classes might promote the usability of HRI results for local stakeholders. The optimal spatial HRI resolution also needs further investigation. While this study used a 100 m × 100 m grid, this may not represent the ideal resolution for HRIs. Future work should explore whether lower or higher resolutions are more effective, incorporating feedback from municipalities actively using HRIs. Further research could also investigate whether HRIs can be developed on a larger scale, spanning multiple countries with a focus on border regions. Also, the integration of additional data and tools might improve HRI accuracy. We followed an open-source approach for all tools and data to ensure accessibility for municipalities. While this improves transparency, it excludes some data and tools that could provide a more accurate representation of reality. Future studies should explore which additional data could be integrated into HRIs. Hazard data could be enhanced by including various climatic indicators or perceived temperatures rather than solely relying on LST, though this would require a comprehensive and widely available monitoring network, which is time- and cost-intensive. In this study, LST represented the annual mean for 2013–2024; however, future research could examine seasonal variations in heat risk by comparing HRI outcomes derived from different seasonal LST averages to better capture temporal and seasonal dynamics. Also, incorporating further indicators such as NDVI can help producing a more holistic HRI. Another important topic relates to weighting approaches in HRI construction. In the current literature different research designs on weighting in HRI constructions can be found such as conducting principal component analysis (PCA) (e.g. [Nayak et al., 2018](#)) or Analytic Hierarchy Process (AHP) (e.g. [Wu et al., 2022](#)). Few studies incorporated interpolation or models to establish an HRI ([Boumans et al., 2014](#); [Quesada-Ganuza et al., 2023](#)). Assigning equal weights to hazard, exposure and sensitivity index in HRI construction is common in the current literature (e.g. [Hu et al., 2017](#); [Mitchell and Chakraborty, 2015](#)). Another important aspect is the weighting of indices within each index, particularly the sensitivity index, which warrants further investigation in future research. Validation with health data, such as mortality and hospitalization records, could strengthen the reliability of the HRI, highlight the urgency of spatially informed heat risk management, and help identify potential risk areas not captured by the current index. Further research is needed to explore how HRIs can be applied in practice to maximize their value for decision-making and planning. Transforming classes into personas to make them more relatable for stakeholders requires further data collection and research. Face-to-face interviews with sample households or detailed, broadly distributed questionnaires could provide richer persona profiles. By creating personas, households and inhabitants are given names, needs, and preferences, facilitating discourse among stakeholders. Participants could track when and where they require heat adaptation or mitigation measures and indicate which measures they prefer. Simultaneously collecting demographic data would allow for more concrete assumptions about which vulnerable groups benefit most from specific strategies. Finally, the link between heat risk management and climate justice needs to be addressed. In the recent years, climate justice in disaster risk management – including heat risk management – has increasingly gained attention in scientific literature (e.g. [Hamdanieh et al., 2024](#); [Pappalardo et al., 2023](#)). Future research could build on the HRI approach by examining how climate justice principles can be incorporated further into heat risk assessment and adaptation planning. Evaluating how the inclusion of social and demographic factors influences the equity and outcomes of adaptation measures could provide valuable insights for just and inclusive heat risk management.

5. Conclusion

Managing heat risk in urban areas will become increasingly important in the coming years, as extreme heat events are expected to increase globally in intensity, frequency, and duration. This will, in turn, enhance the risk for individuals to suffer from heat-related mental as well as physical health issues. These health complications are influenced by a variety of factors, including climatological, physiological, and social ones. HRIs have been established in the scientific literature to identify high heat risk spots. In this study an HRI was established by following the risk triangle approach promoted by the IPCC. This approach combines a hazard index (here: LST), an exposure index (here: population) and a sensitivity index (here: set of census data representing social vulnerability) to form an index

representing heat risk more accurately.

For addressing RG1, this study established an HRI for the three involved model cities Augsburg (Bavaria), Hamm (North-Rhine-Westphalia) and Zwickau (Saxony) to identify heat risk spots. Furthermore, RG2 was tackled by identifying different population groups in all three cities by using an LCA approach to determine subgroups within heat-risk-related census datasets. To ease the reproducibility of this methodological approach all data and tools aimed to be open-source. Similar LCs were detected in all three cities, which led to the creation of three overarching classes: (OC1: “Young & Diverse”, OC2: “Adults & Citizens” and OC3: “Elderly & Single-Household”). These classes formed spatial clusters throughout the cities, with OC1: “Young & Diverse” primarily located in city centres and city quarter centres, OC2: “Adults & Citizens” mostly found in the city outskirts and outer city quarters, and OC3: “Elderly & Single-Household” forming several hotspots across the city area. Furthermore, the different classes showed a different distribution in their HRI with OC1: “Young & Diverse” exhibiting higher HRI values than OC2: “Adults & Citizens” and OC3: “Elderly & Single-Household”. By comparing HRI values with previously established population subgroups it was investigated in which way the population groups identified previously are affected by individual heat stress within the urban environment of each model city.

In the context of this study several maps were established for each model city: a hazard map, an exposure map, a sensitivity map, a population class map as well as an HRI map. Also, all resulting maps are within a 100 m × 100 m resolution as predefined by the available census data. These results might be useful tools for stakeholders in heat risk management and city planning, especially when combining HRI maps with population group maps, which allows for target-oriented planning of heat risk management measures. While adding to RQ2, this might help cities to mitigate their inhabitants' heat risk in a more cost- and time-effective manner. However, both methodological approaches used in this study entail uncertainties and the risk of not accurately depicting reality. Nevertheless, visualizing possible patterns helps in understanding a city's needs for different and target-group-oriented heat risk management. Further research might engage in adapting the heat risk maps according to the in-situ population rather than the de jure population or compare heat risk during different seasons as well as comparing day and night heat risk. Creating detailed personas instead of broad population groups by engaging with the public via interviews might also inhibit benefits for heat risk management in the future.

CRediT authorship contribution statement

Saskia Rupp: Writing – original draft, Visualization, Validation, Methodology, Formal analysis, Data curation, Conceptualization. **Tobias Leichtle:** Writing – review & editing, Data curation, Conceptualization. **Christoph Beck:** Writing – review & editing, Supervision, Funding acquisition, Conceptualization. **Michael Hiete:** Writing – review & editing, Supervision, Funding acquisition, Conceptualization.

Declaration of competing interest

The authors declare that they have no known competing financial interests or personal relationships that could have appeared to influence the work reported in this paper.

Acknowledgments

This study was partly funded by the Federal Ministry for the Environment, Climate Action, Nature Conservation and Nuclear Safety (BMUKN) (Project: “HEATS – Hitzerisikomanagement in der Stadt”, funding code: 67DAS255).

The authors would like to thank the environmental offices of Augsburg, Hamm and Zwickau for their support.

Appendix A. Supplementary data

Supplementary data to this article can be found online at <https://doi.org/10.1016/j.uclim.2025.102769>.

Data availability

Data will be made available on request.

References

Abrar, R., Sarkar, S.K., Nishtha, K.T., Talukdar, S., Shahfahad, Rahman, A., Islam, A.R.M.T., Mosavi, A., 2022. Assessing the spatial mapping of heat vulnerability under urban heat island (UHI) effect in the Dhaka metropolitan area. *Sustainability* 14 (9), 4945.

Adjei, M.J., Yamba, E.I., Tuholske, C., Wemegah, C.S., Amekudzi, L.K., 2025. Assessing heat-related health risk in Ghana using bioclimatic indices. *Sci. Afr.* e02926.

Alonso, L., Renard, F., 2020. A comparative study of the physiological and socio-economic vulnerabilities to heat waves of the population of the metropolis of Lyon (France) in a climate change context. *Int. J. Environ. Res. Public Health* 17 (3), 1004.

Barnes, A., Islam, M.M., Toma, L., 2013. Heterogeneity in climate change risk perception amongst dairy farmers: A latent class clustering analysis. *Appl. Geogr.* 41, 105–115.

Bernhard, M.C., Kent, S.T., Sloan, M.E., Evans, M.B., McClure, L.A., Gohlke, J.M., 2015. Measuring personal heat exposure in an urban and rural environment. *Environ. Res.* 137, 410–418.

Birkmann, J., Jamshed, A., McMillan, J.M., Feldmeyer, D., Totin, E., Solecki, W., Ibrahim, Z.Z., Roberts, D., Kerr, R.B., Poertner, H.-O., 2022. Understanding human vulnerability to climate change: A global perspective on index validation for adaptation planning. *Sci. Total Environ.* 803, 150065.

Bodoque, J.M., Amérigo, M., Díez-Herrero, A., García, J.A., Cortés, B., Ballesteros-Cánovas, J.A., Olcina, J., 2016. Improvement of resilience of urban areas by integrating social perception in flash-flood risk management. *J. Hydrol.* 541, 665–676.

Boumans, R.J., Phillips, D.L., Victery, W., Fontaine, T.D., 2014. Developing a model for effects of climate change on human health and health–environment interactions: heat stress in Austin, Texas. *Urban Clim.* 8, 78–99.

Buscail, C., Upegui, E., Viel, J.-F., 2012. Mapping heatwave health risk at the community level for public health action. *Int. J. Health Geogr.* 11, 1–9.

Buzási, A., 2022. Comparative assessment of heatwave vulnerability factors for the districts of Budapest, Hungary. *Urban Clim.* 42, 101127.

Chen, Q., Din, M., Yang, X., Hu, K., Qi, J., 2018. Spatially explicit assessment of heat health risk by using multi-sensor remote sensing images and socioeconomic data in Yangtze River Delta, China. *Int. J. Health Geogr.* 17 (1). <https://doi.org/10.1186/s12942-018-0135-y>.

Cheng, J., Xu, Z., Bambrick, H., Su, H., Tong, S., Hu, W., 2018. Heatwave and elderly mortality: an evaluation of death burden and health costs considering short-term mortality displacement. *Environ. Int.* 115, 334–342.

Cheng, W., Li, D., Liu, Z., Brown, R.D., 2021. Approaches for identifying heat-vulnerable populations and locations: A systematic review. *Sci. Total Environ.* 799, 149417.

Coid, J.W., Zhang, Y., Yu, H., Li, X., Tang, W., Wang, Q., Deng, W., Guo, W., Zhao, L., Ma, X., 2021. Confirming diagnostic categories within a depression continuum: testing extra-linearity of risk factors and a latent class analysis. *J. Affect. Disord.* 279, 183–190.

Crichton, D., 1999. The risk triangle. *Nat. Disast. Manage.* 102 (3), 102–103.

Cui, Y., Yin, M., Cheng, X., Tang, J., He, B.-J., 2024. Towards cool cities and communities: preparing for an increasingly hot future by the development of heat-resilient infrastructure and urban heat management plan. *Environ. Technol. Innovation* 34, 103568.

Depietri, Y., Welle, T., Renaud, F.G., 2013. Social vulnerability assessment of the Cologne urban area (Germany) to heat waves: links to ecosystem services. *Int. J. Disast. Risk Reduct.* 6, 98–117.

DEUTSCHER WETTERDIENST (DWD), 2025. Climate Data Center. Version v2.1.b22.09. <https://cdc.dwd.de/portal/>.

Dong, J., Peng, J., He, X., Corcoran, J., Qiu, S., Wang, X., 2020. Heatwave-induced human health risk assessment in megacities based on heat stress-social vulnerability-human exposure framework. *Landscape. Urban Plan.* 203, 103907.

Dumont, C.R., Mathis, W.S., 2023. Mapping heat vulnerability of a community mental health center population. *Community Ment. Health J.* 59 (7), 1330–1340.

EARTH RESOURCES OBSERVATION AND SCIENCE (Eros) Center, 2020. Landsat 8–9 Operational Land Imager / Thermal Infrared Sensor Level-2, Collection 2 [Dataset]. Geological Survey, U.S. <https://doi.org/10.5066/P90GBGM6>.

Ebi, K.L., Capon, A., Berry, P., Broderick, C., DE Dear, R., Havenith, G., Honda, Y., Kovats, R.S., Ma, W., Malik, A., 2021. Hot weather and heat extremes: health risks. *Lancet* 398 (10301), 698–708.

Ellena, M., Melis, G., Zengarini, N., Di Gangi, E., Ricciardi, G., Mercogliano, P., Costa, G., 2023. Micro-scale UHI risk assessment on the heat-health nexus within cities by looking at socio-economic factors and built environment characteristics: the Turin case study (Italy). *Urban Clim.* 49, 101514.

European Environment Agency, 2022. Climate Change as a Threat to Health and Well-Being in Europe: Focus on Heat and Infectious Diseases. Copenhagen.

Ferguson, M., Mohamed, M., Higgins, C.D., Abotalebi, E., Kanaroglou, P., 2018. How open are Canadian households to electric vehicles? A national latent class choice analysis with willingness-to-pay and metropolitan characterization. *Transp. Res. Part D: Transp. Environ.* 58, 208–224.

Forceville, G., Lemonsu, A., Goria, S., Stempflet, M., Host, S., Alessandrini, J.-M., Cordeau, E., Pascal, M., 2024. Spatial contrasts and temporal changes in fine-scale heat exposure and vulnerability in the Paris region. *Sci. Total Environ.* 906, 167476.

Frasch, J.J., König, H.-H., Konnopka, C., 2025. Effects of extreme temperature on morbidity, mortality, and case severity in German emergency care. *Environ. Res.* 121021.

Friesenecker, M., Schneider, A., Bügelmayer-Blaschek, M., Getzner, M., Hahn, C., Schneider, M., Seebauer, S., Zawadzki, W., Zuvela-Aloise, M., Thaler, T., 2025. Socially equitable climate risk management of urban heat. *npj Urban Sustain.* 5 (1), 8. <https://doi.org/10.1038/s42949-025-00202-2>.

Georgy, S., Lautenbach, S., Jahn, H.J., Katschner, L., Krämer, A., 2019. Erfassung von hitze- und feinstaubbedingten Gesundheitsrisiken in Deutschland: Ein epidemiologischer Studienansatz. *Bundesgesundheitsblatt-Gesundheitsforschung-Gesundheitsschutz* 62 (6).

GERMAN FEDERAL MINISTRY FOR HOUSING, URBAN DEVELOPMENT AND BUILDING, 2017. Hamm-Norden Schottschleife/Schlagenkamp. Hamm, Germany. https://www.nationale-stadtentwicklungspolitik.de/NSP/SharedDocs/Projekte/WSProjekte_DE/Hamm_Norden_Schottschleife_Schlagenkamp.html.

German Federal Statistics Office, 2024a. Census 2022. Wiesbaden, Germany. https://www.zensus2022.de/DE/Aktuelles/Hinweis_Zensusatlas.html?nn=270470.

German Federal Statistics Office, 2024b. Census 2022. Wiesbaden, Germany [dataset]. https://www.zensus2022.de/DE/Ergebnisse-des-Zensus/_inhalt.html.

Guardaro, M., Hondula, D.M., Redman, C.L., 2022. Social capital: improving community capacity to respond to urban heat. *Local Environ.* 27 (9), 1133–1150. <https://doi.org/10.1080/13549839.2022.2103654>.

Hamdanieh, L., Stephens, C., Olyaeemanesh, A., Ostadtaghizadeh, A., 2024. Social justice: the unseen key pillar in disaster risk management. *Int. J. Disast. Risk Reduct.* 101, 104229.

Hammer, J., Ruggieri, D.G., Thomas, C., Caum, J., 2020. Local extreme heat planning: an interactive tool to examine a heat vulnerability index for Philadelphia, Pennsylvania. *J. Urban Health* 97, 519–528.

Hass, A.L., Ellis, K.N., 2019. Motivation for heat adaption: how perception and exposure affect individual behaviors during hot weather in Knoxville, Tennessee. *Atmosphere* 10 (10), 591.

Herrmann, A., Sauerborn, R., 2018. General practitioners' perceptions of heat health impacts on the elderly in the face of climate change—A qualitative study in Baden-Württemberg, Germany. *Int. J. Environ. Res. Public Health* 15 (5), 843.

Ho, H.C., Tong, S., Zhou, Y., Hu, K., Yang, X., Yang, Y., 2025. Mapping heat vulnerability and heat risk for Neighborhood health risk Management in Urban Environment? Challenges and opportunities. *Curr. Environ. Health Rep.* 12 (1), 14. <https://doi.org/10.1007/s40572-025-00478-7>.

Howe, P.D., Leiserowitz, A., 2013. Who remembers a hot summer or a cold winter? The asymmetric effect of beliefs about global warming on perceptions of local climate conditions in the U.S. *Glob. Environ. Chang.* 23 (6), 1488–1500. <https://doi.org/10.1016/j.gloenvcha.2013.09.014>.

Hu, K., Yang, X., Zhong, J., Fei, F., Qi, J., 2017. Spatially explicit mapping of heat health risk utilizing environmental and socioeconomic data. *Environ. Sci. Technol.* 51 (3), 1498–1507. <https://doi.org/10.1021/acs.est.6b04355>.

Hua, J., Zhang, X., Ren, C., Shi, Y., Lee, T.-C., 2021. Spatiotemporal assessment of extreme heat risk for high-density cities: A case study of Hong Kong from 2006 to 2016. *Sustain. Cities Soc.* 64, 102507.

Huang, X., Li, Y., Guo, Y., Zheng, D., Qi, M., 2020. Assessing urban risk to extreme heat in China. *Sustainability* 12 (7), 2750.

INTERGOVERNMENTAL PANEL ON CLIMATE CHANGE, 2023. Summary for policymakers. In: Lee, H., Romero, J. (Eds.), Climate Change 2023: Synthesis Report. IPCC, Geneva, Switzerland, pp. 1–34.

Jay, O., Capon, A., Berry, P., Broderick, C., DE Dear, R., Havenith, G., Honda, Y., Kovats, R.S., Ma, W., Malik, A., 2021. Reducing the health effects of hot weather and heat extremes: from personal cooling strategies to green cities. *Lancet* 398 (10301), 709–724.

Kácha, O., Vintr, J., Brick, C., 2022. Four Europes: climate change beliefs and attitudes predict behavior and policy preferences using a latent class analysis on 23 countries. *J. Environ. Psychol.* 81, 101815.

Kántor, N., Chen, L., Gál, C.V., 2018. Human-biometeorological significance of shading in urban public spaces—summertime measurements in Pécs, Hungary. *Landscape. Urban Plan.* 170, 241–255.

Keller, A., Groot, J., Clippert-Jensen, C., Pinot De Moira, A., Pedersen, M., Sigsgaard, T., Loft, S., Budtz-Jørgensen, E., Nybo Andersen, A.-M., 2024. Exposure to different residential indoor characteristics during childhood and asthma in adolescence: A latent class analysis of the Danish National Birth Cohort. *Eur. J. Epidemiol.* 39 (1), 51–65.

Kenny, G.P., Yardley, J., Brown, C., Sigal, R.J., Jay, O., 2010. Heat stress in older individuals and patients with common chronic diseases. *Cmaj* 182 (10), 1053–1060.

Kiefer, S., Bachmeir, M., 2017. Sozialbericht der Stadt Augsburg 2017. Stadt Augsburg, Sozialreferat.

Klopfen, F., Pfeiffer, A., 2023. Determining spatial disparities and similarities regarding heat exposure, green provision, and social structure of urban areas-A study on the city district level in the Ruhr area, Germany. *Heliyon* 9 (6).

Korkala, E.A., Hugg, T.T., Jaakkola, J.J., 2014. Voluntary climate change mitigation actions of young adults: A classification of mitigators through latent class analysis. *PLoS One* 9 (7), e102072.

Kumar, P., Debele, S.E., Khalili, S., Halios, C.H., Sahani, J., Aghamohammadi, N., de Andrade, M.F., Athanassiadou, M., Bhui, K., Calvillo, N., Cao, S.-J., Coulon, F., Edmondson, J.L., Fletcher, D., Dias De Freitas, E., Guo, H., Hort, M.C., Kattt, M., Kjeldsen, T.R., Jones, L., 2024. Urban heat mitigation by green and blue infrastructure: drivers, effectiveness, and future needs. *Int. J. Hydrogen Energ.* 5 (2), 100588. <https://doi.org/10.1016/j.ijhydene.2024.100588>.

Leichtle, T., Helgert, S., Müller, M., Handschuh, J., Erbertseder, T., Wurm, M., Taubenböck, H., 2023a. Opposing Land Surface and Air Temperatures From Remote Sensing and Citizen Science for Quantification of the Urban Heat Island Effect, pp. 1–5.

Leichtle, T., Kühnl, M., Droin, A., Beck, C., Hiete, M., Taubenböck, H., 2023b. Quantifying urban heat exposure at fine scale-modeling outdoor and indoor temperatures using citizen science and VHR remote sensing. *Urban Clim.* 49, 101522.

Liao, Q., Yuan, J., Lam, W.W.T., Lee, T., Yang, L., Tian, L., Fielding, R., 2024. Climate change scepticism and its impacts on individuals' engagement with climate change mitigation and adaptation to heat in Hong Kong: A two-wave population-based study. *J. Environ. Psychol.* 94, 102251.

Linzer, D.A., Lewis, J.B., 2011. poLCA: An R package for polytomous variable latent class analysis. *J. Stat. Softw.* 42, 1–29.

Linzer, D.A., Lewis, J.B., 2013. poLCA: Polytomous Variable Latent Class Analysis. R Package Version, 1, p. 4. <https://dlinzer.github.com/poLCA>.

Masselot, P., Mistry, M.N., Rao, S., Huber, V., Monteiro, A., Samoli, E., Stafoggia, M., De'donato, F., Garcia-Leon, D., & Ciscar, J.-C., 2025. Estimating future heat-related and cold-related mortality under climate change, demographic and adaptation scenarios in 854 European cities. *Nat. Med.* 1–9.

Ministry Of Internal Affairs, 2022. Sicherheitsanalyse Zwickau: Analyse zur objektiven Lage sowie zum Sicherheits- und Zufriedenheitsgefühl der Bürgerinnen und Bürger im Rahmen der "Allianz sichere Sächsische Kommunen". ASSKOMM.

Mitchell, B.C., Chakraborty, J., 2015. Landscapes of thermal inequity: disproportionate exposure to urban heat in the three largest US cities. *Environ. Res. Lett.* 10 (11). <https://doi.org/10.1088/1748-9326/10/11/115005>.

Mohammed, A.M., 2025. The heat adaptation priority index (HAPI): A practical tool for urban heat risk assessment and mitigation priority. *Sustain. Cities Soc.* 106420.

Nayak, S.G., Shrestha, S., Kinney, P.L., Ross, Z., Sheridan, S.C., Pantea, C.I., et al., 2018. Development of a heat vulnerability index for New York state. *Public Health* 161, 127–137. <https://doi.org/10.1016/j.puhe.2017.09.006>.

Nguyen, T.N.P., Hunsberger, M., Löve, J., Duong, T.A., Phan, T.H., Luong, N.K., Hoang, V.M., Ng, N., 2024. Patterns and determinants of tobacco purchase behaviors among male cigarette smokers in Vietnam: A latent class analysis. *Tob. Induc. Dis.* 22, 10–18332.

Pappalardo, S.E., Zanetti, C., Todeschi, V., 2023. Mapping urban heat islands and heat-related risk during heat waves from a climate justice perspective: A case study in the municipality of Padua (Italy) for inclusive adaptation policies. *Landsc. Urban Plan.* 238, 104831.

Park, J., Kim, J.-H., Sohn, W., Li, M.-H., 2022. Cooling ranges for urban heat mitigation: continuous cooling effects along the edges of small greenspaces. *Landsc. Ecol. Eng.* 1–13.

Paterson, S.K., Godsmark, C.N., 2020. Heat-health vulnerability in temperate climates: lessons and response options from Ireland. *Glob. Health* 16, 1–17.

Pinchoff, J., Mahapatra, B., Mishra, R., Adedimeji, A., Patel, S.K., Regules, R., 2024. Classifying climate vulnerability and inequalities in India, Mexico, and Nigeria: A latent class analysis approach. *Environ. Res. Lett.* 19 (3), 034009.

Quesada-Ganuza, L., Garmendia, L., Alvarez, I., Roji, E., 2023. Vulnerability assessment and categorization against heat waves for the Bilbao historic area. *Sustain. Cities Soc.* 98, S. 104805. <https://doi.org/10.1016/j.scs.2023.104805>.

Roberts, E., Sun, T., Pelling, M., 2025. Compound Urban Heat Risk Revealed by Co-Location of Social Vulnerability and Elevated Temperatures in London, UK. A spatial analysis. *Sustainable Cities and Society*, p. 106756.

Sadeghi, M., Chaston, T., Hanigan, I., DE Dear, R., Santamouris, M., Jalaludin, B., Morgan, G.G., 2022. The health benefits of greening strategies to cool urban environments—A heat health impact method. *Build. Environ.* 207, 108546.

Saucy, A., Ragettli, M.S., Vienneau, D., DE Hoogh, K., Tangermann, L., Schäffer, B., Wunderli, J.-M., Probst-Hensch, N., Röösli, M., 2021. The role of extreme temperature in cause-specific acute cardiovascular mortality in Switzerland: A case-crossover study. *Sci. Total Environ.* 790, 147958.

Seebaß, K., 2017. Who is feeling the heat?: vulnerabilities and exposures to heat stress—individual, social, and housing explanations. *Nat. Cult. 12* (2), 137–161.

Sinha, P., Calfee, C.S., Delucchi, K.L., 2021. Practitioner's guide to latent class analysis: methodological considerations and common pitfalls. *Crit. Care Med.* 49 (1), e63–e79.

Sun, Y., Li, Y., Ma, R., Gao, C., Wu, Y., 2022. Mapping urban socio-economic vulnerability related to heat risk: A grid-based assessment framework by combining the geospatial big data. *Urban Clim.* 43, 101169.

Susca, T., Zanghirella, F., Colasunno, L., DEL Fatto, V., 2022. Effect of green wall installation on urban heat island and building energy use: A climate-informed systematic literature review. *Renew. Sustain. Energy Rev.* 159, 112100.

Wang, J., Nikolaou, N., An Der Heiden, M., Irgang, C., 2024. High-resolution modeling and projection of heat-related mortality in Germany under climate change. *Commun. Med.* 4 (1), 206. <https://doi.org/10.1038/s43856-024-00643-3>.

Weller, B.E., Bowen, N.K., Faubert, S.J., 2020. Latent class analysis: A guide to best practice. *J. Black Psychol.* 46 (4), 287–311.

Wolf, J., Adger, W.N., Lorenzoni, I., Abrahamson, V., Raine, R., 2010. Social capital, individual responses to heat waves and climate change adaptation: an empirical study of two UK cities. *Glob. Environ. Chang.* 20 (1), 44–52.

Wu, C., Shui, W., Huang, Z., Wang, C., Wu, Y., Xue, C., et al., 2022. Urban heat vulnerability: a dynamic assessment using multi-source data in coastal metropolis of Southeast China. *Front. Publ. Health* 10. <https://doi.org/10.3389/fpubh.2022.989963>.

Xiang, Z., Qin, H., He, B.-J., Han, G., Chen, M., 2022. Heat vulnerability caused by physical and social conditions in a mountainous megacity of Chongqing, China. *Sustain. Cities Soc.* 80, 103792.

Zhang, C., Yang, Y., Yu, L., 2025. Assessing urban surface thermal environment and heat health risk in Chinese cities: a twenty-year study. *Urban Clim.* 59, 102304.